Nat. Hazards Earth Syst. Sci. Discuss., https://doi.org/10.5194/nhess-2017-330
Manuscript under review for journal Nat. Hazards Earth Syst. Sci.
Discussion started: 12 October 2017

Natural Hazards and Earth System Sciences
Discussions

Development of bridge failure model and fragility curves for infrastructure overturning and deck sliding due to lahars

Joaquín Dagá[1], Alondra Chamorro[2], Hernán de Solminihac[3], Tomás Echaveguren[4]

[1]Master Student of Engineering Sciences, Department of Engineering and Construction Management, Faculty of Engineering, Pontificia Universidad Católica de Chile, Santiago, Chile.
[2]Associate Professor, School of Engineering, Pontificia Universidad Católica de Chile. Research Associate, National Research Center for Integrated Disaster Risk Management (CIGIDEN), Santiago, Chile.
[3]Professor, School of Engineering, Pontificia Universidad Católica de Chile. Director of the Engineering and Construction Management Department, School of Engineering, Pontificia Universidad Católica de Chile. Planning Director of the Latin American Center of Economic and Social Policies UC (CLAPES UC), Santiago, Chile.
[4]Associate Professor, Civil Engineering Department, Faculty of Engineering, Universidad de Concepción. Researcher, National Research Center for Integrated Disaster Risk Management (CIGIDEN), Concepción, Chile.

Correspondence to: Joaquín Dagá (jadaga@uc.cl)

Abstract. One of the main volcanic processes affecting road infrastructure are lahars, which are flows of water and volcanic material running down the slopes of a volcano and river valleys. Empirical evidence has shown that lahars generate permanent deterioration in bridges and culverts, however, no models are available to estimate failure probability and vulnerability of these structures exposed to this hazard. In this paper, a bridge failure model due to lahars is proposed and, based on this, fragility curves for infrastructure overturning and deck sliding are developed. The failure model considers the limit state of infrastructure overturning moment and the tangential force over the deck caused by lahars, considering bridges with and without piers. Analytical models to estimate these loads were calibrated to simulate the effect of lahars over bridges for the development of fragility curves. Monte Carlo was applied to simulate the probability of failure given by different lahar depths, which is a continuous variable correlated to other lahar flow characteristics, such as velocity and scour demand. Fragility curves of bridges were parameterized by maximum likelihood estimation, using a cumulative lognormal distribution. Parametrized fragility curves were successfully validated for a 95 % confidence level using data of 14 bridges that were reached by lahars in the last 50 years. Validated models confirm that decks fail mainly due to piers and/or abutment overturning rather than sliding forces. Moreover, it was concluded that bridges with piers are more vulnerable to lahars. The developed models can be applied to existing and new bridges exposed to volcanic hazards to estimate the failure probability given an expected lahar intensity. Further research is being conducted to develop an application tool to simulate the effects of expected lahars in existing bridges of a road network.

1 Introduction

Volcanic eruptions generate operational losses and permanent physical damage in road infrastructure, as evidenced by historical data regarding this natural hazard. The level of damage depends on the infrastructure's exposure and vulnerability

as well as the type of volcanic event, namely: pyroclastic fall, pyroclastic flow, lava flow and lahar. Consequences related to pyroclastic fall, specifically tephra, are temporary road closures due to lack of visibility and surface friction loss (Nairn, 2002; Leonard et al., 2005; Wilson et al., 2012). Lava and pyroclastic flows destroy the entire reached infrastructure; however, its probability of occurrence and area of affection is lower (Wilson et al., 2014). This implies less exposure and, therefore, vulnerability of the infrastructure to these two events. Lahars, which are flows of water, rock fragments and debris running down the slopes of a volcano and river valleys, affect both operationally and physically road infrastructure (Smith and Fritz, 1989). Volcanic debris and sediments transported by lahars make these flows especially destructive. In addition, these flows produce scour on the riverbed, permanently damaging exposed infrastructure (Vallance and Iverson, 2015; Muñoz-Salinas et al., 2007; Nairn, 2000). Wilson et al. (2014) demonstrated that critical infrastructure affected by lahars are bridges (including piers, foundations, abutments and deck) and culverts. For example, as a consequence of Mount St. Helens (USA) eruption in 1980, 300 km of highways were damaged where 48 bridges were affected (Blong, 1984; Wilson et al., 2014). Moreover, two volcanic eruptions occurred in Chile in 2015 (Villarrica and Calbuco volcanoes) resulted in the collapse of four bridges out of six reached by lahars.

The probability of failure of an infrastructure given a certain natural hazard can be estimated considering calibrated fragility curves, which are commonly integrated in available modelling tools. For example, in the United States the Federal Emergency Management Agency (FEMA) developed HAZUS-MH tool for risk management of structures and infrastructure. This GIS-based software studies three natural hazards: earthquakes, floods and hurricanes, excluding the volcanic hazard from the analysis (FEMA, 2011). Likewise, the RiskScape software developed by the National Institute of Water and Atmospheric Research (NIWA) account for the effects of earthquakes, tsunamis, floods, hurricanes and volcanic eruptions over assets. Nevertheless, the effects of volcanoes are only accounted in terms of ash fall and the temporary effects on infrastructure operation (Kaye, 2008).

From available literature and the current state-of-the-practice, it is concluded that no failure models and fragility curves have been developed to estimate bridge failure probability due to lahar flows. The main objective of the study is to propose a bridge failure model and develop bridge fragility curves due to lahars, considering piers and abutments overturning, as well as, deck sliding. Models development consider the calibration, parametrization and validation of bridge fragility curves due to lahars based on a limit state model. Two types of bridges are considered in the analysis, this is, bridges with and without piers.

The research starts with the characterization of the lahar process and the physical effects on bridges. A failure model is then proposed considering the limit state of infrastructure overturning moment and the tangential force over the deck caused by lahars, considering bridges with and without piers. An experimental design is consistently defined to calibrate fragility curves based on analytical models that characterize the effect of lahars over bridges. Monte Carlo simulations are applied to estimate the probability of failure given by different lahar depths. Fragility curves of bridges are then parameterized by maximum likelihood estimation, using a cumulative lognormal distribution. Finally, fragility curves are empirically validated from historical data and resulting curves are analyzed in detail.

Nat. Hazards Earth Syst. Sci. Discuss., https://doi.org/10.5194/nhess-2017-330
Manuscript under review for journal Nat. Hazards Earth Syst. Sci.
Discussion started: 12 October 2017

Natural Hazards and Earth System Sciences
Discussions

2 Characterization of lahars for fragility curves development

2.1 Physical description of lahar flows

Lahars are high-velocity flows composed of volcanic debris and water, travelling through ravines and riverbeds (Pierson et al., 2009). Lahar flows are originated by a violent melting of snow and/or ice caused by the heat flow derived from lavas or pyroclastic flows issued during a volcanic event, or by avalanches of non-consolidated volcanic material during intense rains or violent rupture of a lake or pond (Waitt, 2013). Lahars are categorized according to their sediment/water ratio (Smith and Fritz, 1989). On one hand, there are debris flows, highly viscous slurries of sediment and water. They are capable of transporting gravel-sized in suspension, and their concentration of solid particles ranges between 75 and 80 % in weight or 55 and 60 % in volume. On the other hand, there are hyper-concentrated flows, which have high suspended fine contents, predominantly due to fluid motion and properties. Their solid concentrations reaches 55 to 60 % in weight and 35 to 40 % in volume (Pierson et al., 2009).

As for their geographical scope, lahars flow guided by gravity, so they are capable of impacting elements located tens of kilometers away from the crater of the volcano (Parfitt and Wilson, 2008). Furthermore, these flows can reach velocities up to 140 km/h, as observed in Mt. Saint Helens in the United States in 1980 (Pierson, 1985). The velocity and composition of lahars make these flows destructive.

According to Vallance and Iverson (2015), and Bono (2014), the most important eruptive processes in a lahar are the erosion of the steep slopes and fluvial terraces by scouring their beds. Being more significant the erosion observed in steeper river valleys with weaker beds. Watery sediment floods are more erosive than sediment-rich flows, where scour of the riverbed drags massive material blocks (presenting diameters over 10 m) and vegetation. In this context, bridges in volcanic areas mostly located in affected valleys. The scour that these flows generate in the bed, together with the associated loads of high velocity lahars and the impact of debris travelling with them, may cause the collapse or permanent deterioration of bridges (Nairn, 2002). This explains in part the high vulnerability bridges due to lahar flows.

The destructive potential of a lahar affecting a bridge depends on the season in which they occur, the existence of a glacier, rainfall and the prevailing temperatures during winter. The destructive potential of a lahar increases when the eruption occurs at the end of the winter, since in this period of the year there is more accumulated snow, compacted in layers, and more volume of ice melting. This condition is enhanced if winter temperatures were low, because greater volumes of ice and snow melting may increase lahars intensity (Moreno, 2015).

2.2 Bridge fragility curves for lahar risk modeling

In order to incorporate the uncertainty of the characteristics of lahar flows and the bridge engineering design (X), it is proposed to quantify the bridge failure probability due to lahars by using fragility curves. The latter express the probability that a system exceeds different damage states (ds_i) in function of the hazard intensity measure (IM). Thus, they allow

Nat. Hazards Earth Syst. Sci. Discuss., https://doi.org/10.5194/nhess-2017-330
Manuscript under review for journal Nat. Hazards Earth Syst. Sci.
Discussion started: 12 October 2017

Natural Hazards and Earth System Sciences
Discussions
Open Access
EGU

quantifying the failure probability of a system due to an event of a specific intensity (Rossetto et al., 2013). In this way, fragility curves reflect the system's vulnerability to the studied natural hazard.

$$P(DS \geq ds_i | IM) \,, \tag{1}$$

Schulz et al. (2010) define four approaches for developing a system's fragility curves. First, there is the empirical approach, which is based on historical data and/or experiments. On the other hand, curves can be based on experts' opinion. They can also be developed using an analytical approach through models that characterize the limit state of the element, based on probabilistic and deterministic variables defining the system. Finally, a hybrid method, which combines two or more of the recently described approaches, can be used.

Since there are no existing models addressing lahar risk on bridges, a challenge for the development of bridge fragility curves due to lahars consists in defining a unique hazard intensity measure (IM). In the flood module of the HAZUS-MH software, the Federal Emergency Management Agency developed fragility curves using the flow depth to quantify the hazard intensity (FEMA, 2011). Tsubaki et al. (2016) use the same variable for measuring the flood intensity when developing embankment fragility curves. On the other hand, Wilson et al. (2014) propose the flow depth as one of the potential intensity measures for developing fragility curves related to lahar flows. Moreover, the existing velocity and scour models use the flow height as a main variable (Chilean Ministry of Public Works (MOP), 2016; Arneson et al., 2012). Thus, in order to develop bridge fragility curves due to lahars, the use of flow depth is proposed as the intensity measure.

3 Proposed failure model for infrastructure overturning and deck sliding due to lahars

3.1 Conceptual model

In order to model the bridge fragility due to lahars, the analytical approach is used through the reliability theory. The assessment of the bridge reliability in case of lahars can be considered a supply and demand problem associated to this system bridge-lahar. The supply function ($S(X)$) of the bridge corresponds to its capacity to resist the loads of the lahar; therefore it is directly related to the design of the structural element. On the other hand, the demand function ($D(X)$) corresponds to the load applied by the lahar on the bridge. The limit state function ($g(X)$) of the bridge-lahar system is given by the difference between the supply function of the bridge and the demand function of the lahar flow. If this function of the attributes of the lahar and the bridge (X) is less than zero, it means that the lahar loads on the structure are greater than the bridge capacity, hence, the bridge will fail.

In order to define the potential impacts of lahars on a standard bridge, the loads applied by the lahar flow on each bridge component are identified and characterized. With the aim of conceptualizing this analysis, a bridge-lahar model was developed, which is shown in the free-body diagram in Figure 1. It contains the cross section of a bridge, together with the main physical loads applied by the lahar on the bridge. The cross section of the bridge modelled in Fig. 1 is composed by the infrastructure (foundation and pier/abutment) and the superstructure (deck and beams). The proposed model assumes that the

Nat. Hazards Earth Syst. Sci. Discuss., https://doi.org/10.5194/nhess-2017-330
Manuscript under review for journal Nat. Hazards Earth Syst. Sci.
Discussion started: 12 October 2017

Natural Hazards and Earth System Sciences
Discussions

foundation has no piles. Additionally, it assumes that the superstructure is simply supported on piers and abutments.

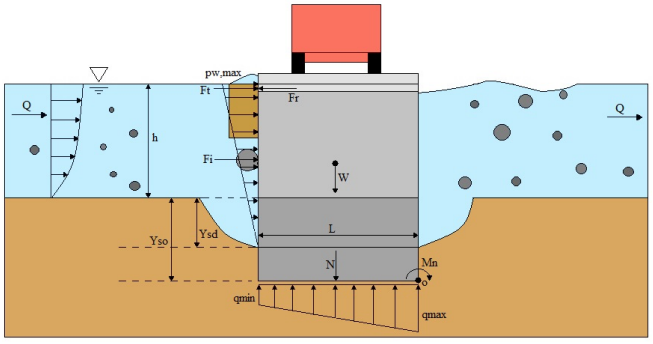

Figure 1: Free Body Diagram of bridge resisting and demanding forces and moments in the presence of a lahar.

Fig. 1 shows a lahar with depth h acting on a bridge of width L and weight W. The foundation of the pier or abutment of the bridge was designed with a depth Y_{so}. This represents the supply or capacity of the bridge due to scour. The foundation transfers loads to the ground, considering a trapezoidal distributed load model. The modelled lahar generates a hydrodynamic pressure p_w, which acts perpendicular to the bridge. This pressure produces a resulting hydrodynamic tangential force F_{wi} on the piers and abutments and a force F_{ws} on the bridge superstructure. The deck of the bridge resists the sliding with a friction force F_r. The lahar also generates a scour demand Y_{sd} on the bed, around the foundation. Furthermore, the debris transported by the lahar colliding with the bridge, impact the structure with a force F_i. All these forces produce a net resulting moment M_n on the lower right vortex of the foundation. This net moment M_n is equal to the difference between the overturning moment M_v generated by hydrodynamic forces F_{wi} and debris impact F_i and the resistant moment produced by the weight W of the bridge.

3.2 Bridge failure mechanisms due to lahars

The hydrodynamic pressure of the lahar flow (p_w) and the impact force of the debris (F_i) can cause the overturning of bridge piers and abutments. This is further enhanced by the scour that these flows generate around the foundations. On the other hand, the same hydrodynamic pressure of the lahars, together with the potential impact of debris, can cause deck sliding.

Therefore, in order to analyze the effects of lahars on bridges, failure mechanisms associated to three bridge components are defined: pier overturning, abutment overturning and sliding of the bridge superstructure. In addition to these failure mechanisms, the access embankment of the bridge may collapse. However, this component is not included in the modelling due to its lower replacement cost in relation to other bridge components. All these failure mechanisms are consistent with the postulates of Wilson et al. (2014) and the records of lahar effects on the eruptions of the Villarrica Volcano and the Calbuco

Nat. Hazards Earth Syst. Sci. Discuss., https://doi.org/10.5194/nhess-2017-330
Manuscript under review for journal Nat. Hazards Earth Syst. Sci.
Discussion started: 12 October 2017

Natural Hazards and Earth System Sciences
Discussions
Open Access
EGU

Volcano in 2015 (MOP, 2015a; MOP, 2015b). Images in Fig. 2 (a) and (b) show the Río Blanco Bridge (Chile) before and after a lahar flow following the eruption of Calbuco volcano in 2015. Fig. 2 shows the structural collapse of the bridge due to the overturning of the pier and subsequent sliding of the deck.

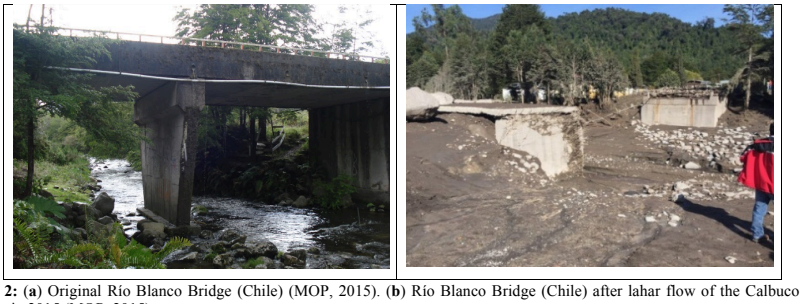

Figure 2: (**a**) Original Río Blanco Bridge (Chile) (MOP, 2015). (**b**) Río Blanco Bridge (Chile) after lahar flow of the Calbuco volcano eruption in 2015 (MOP, 2015).

3.2.1 Infrastructure overturning (piers and abutments)

Both piers and abutments are components susceptible to overturning due to lahars. These dense and fast-travelling flows generate a resulting hydrodynamic force (F_{wi}) on the bridge infrastructure, which entails an overturning moment (M_{wi}). In addition, the impact force (F_i) of the debris on piers and abutments produces the overturning moment (M_i). The bridge weight W generates a moment (M_r) resisting to the infrastructure overturning.

Through equilibrium of moments, considering the turning point O located in the vertex of the foundation, it is possible to evaluate the stability of the bridge piers and abutments in the presence of a lahar flow of a specific intensity. The overturning of piers and abutments is produced if the overturning moment ($M_v = M_{wi} + M_i$) caused by the lahar on the component is greater than the resistant moment (M_r). In other words, the overturning is produced when the net moment (M_n) is less than zero. On the other hand, a lahar can also cause the overturning of piers and abutments when the scour generated by the flow $Y_{sd}(X)$ is greater than the design scour of the infrastructure $Y_{so}(X)$.

Thus, the above allows establishing the limit state function $g_{VI}(X)$ related to the overturning of piers and abutments due to lahars. This function allows quantifying the overturning probability of the infrastructure considering the parameters (X) of the system and the lahar intensity h_1:

$$P_{VI} = P(g_{VI}(X) \leq 0)\,, \tag{2}$$

$$g_{VI}(X) = \min\{M_r(X) - M_v(X);\ Y_{so}(X) - Y_{sd}(X)\}\,, \tag{3}$$

This function indicates that, given a lahar with height h_1, the infrastructure will overturn if the overturning moment M_v is greater than the resistant moment M_r and/or the lahar scour demand Y_{sd} is higher than the design scour of the bridge Y_{so}.

Nat. Hazards Earth Syst. Sci. Discuss., https://doi.org/10.5194/nhess-2017-330
Manuscript under review for journal Nat. Hazards Earth Syst. Sci.
Discussion started: 12 October 2017

Natural Hazards and Earth System Sciences
Discussions

The scour produced by lahar flows near the foundations contribute to a greater vulnerability of these bridge components, since they produce destabilization and weakening around the foundation of piers and abutments. If there is scour in the bed, the foundation of the pier or abutment will be exposed to a higher hydrodynamic pressure. This load is higher in the case of lahars, given their greater density and velocity in relation to normal floods. Thus, a greater scour demand will imply a larger surface affected by the hydrodynamic pressure. In turn, this means a greater resulting hydrodynamic force (F_{wi}) and, therefore, a greater moment associated to this force (M_{wi}).

3.2.2 Deck sliding

In the case where the lahar height exceeds the bridge clearance, the lahar flow will exert a hydrodynamic pressure on the bridge superstructure. There is also the possibility that the debris transported by the lahar flow impacts the bridge deck. This debris impact force (F_i), together with the hydrodynamic force (F_{ws}) can cause failure due to deck sliding. On the other hand, the presence of microscopic imperfections between the contact surfaces of the superstructure and the infrastructure produces a static friction force (F_r).

Through the equilibrium of forces it can be inferred that the deck of a bridge subjected to a lahar will slide if the resulting tangential force ($F_t = F_{ws} + F_i$) is higher than the static friction force (F_r) between the infrastructure and the superstructure. It should be highlighted that this force is zero if the lahar height is lower than the bridge clearance.

This allows establishing the limit state function $g_{DS}(X)$ associated to the superstructure failure due to its potential sliding:

$$P_{DS} = P(g_{DS}(X) \leq 0)\ , \tag{4}$$

$$g_{DS}(X) = F_r(X) - F_t(X)\ , \tag{5}$$

The limit state function defined in Eq. (5) implies that, under attributes X, if the friction force is lower than the tangential force produced by the lahar, the failure mechanism associated to sliding will be activated.

4 Experimental design for modelling infrastructure overturning and deck sliding due to lahars

4.1 Physical models to estimate limit state functions

Once the limit state functions have been analytically defined, the different loads presented in the free-body diagram have to be quantified. Therefore, existing models are used and integrated. First, the lahar velocity (v_{Lahar}) is quantified with the Manning formula, based on the height, as recommended by Cowan (1956) along with Laenen and Hansen (1988).

The lahar scour demand is quantified based on the empirical equation proposed by Arneson et al. (2012). Müller (1996) compared 22 equations proposed in the literature to estimate scour. Therefore, he used empirical data of 384 field measurements of 56 bridges. The conclusion of this study was that the equation proposed by Arneson et al. (2012) in the

Nat. Hazards Earth Syst. Sci. Discuss., https://doi.org/10.5194/nhess-2017-330
Manuscript under review for journal Nat. Hazards Earth Syst. Sci.
Discussion started: 12 October 2017

Natural Hazards and Earth System Sciences
Discussions

Hydraulic Engineering Circular No. 18 (HEC-18) was suitable for quantifying the magnitude of the scour.

On the other hand, the debris transported by the flows are accumulated in the bridge piers, thus creating an additional obstruction to the flow. So, the scour demand on the piers (Y_{c-d}) is modelled with Eq. (6) and (7) of the NCHRP (2010) and Zevenbergen et al. (2007), which considers a triangular or rectangular debris accumulation (K_E) with height H_d and width W_d to estimate an effective widening (b_d^*) of the pier with width b. It should be noted that factors K_1, K_2 and K_3 are correction factors of the pier shape, the flow angle and the bed condition, respectively.

$$Y_{c-d} = h_{Lahar} * 2 * K_1 * K_2 * K_3 * \left(\frac{b}{h_{Lahar}}\right)^{0,65} * {Fr_{Lahar}}^{0,65}, \quad (6)$$

$$b_d^* = \frac{K_E*(H_d*W_d)+(h_{Lahar}-K_E*H_d)*b}{h_{Lahar}}, \quad (7)$$

Regarding the abutments, according to HEC-18, the scour demand on this component (Y_{e-d}) is based on the flow depth, the flow width, the bridge length and a bed condition amplification factor (α).

$$Y_{e-d} = \alpha * h_{Lahar} * \left(\frac{b_{Flow}}{L_{Bridge}}\right)^{6/7} - h_{Lahar}\ , \quad (8)$$

The scour supply is estimated with models adapted from bridge design manuals. For example, Breusers, Nicollet and Shen (1977) stipulate Eq. (9) and (10) to assess the design scour of piers (Y_{c-o}) and abutments (Y_{e-o}). These equations include variables such as design height (h_{design}), pier width (b) and correction factors by flow angle, pier shape, among others:

$$Y_{c-o} = 2 * \left(K_S * K_w * K_g * K_{gr} * K_R * K_d\right) * b * tanh\left(\frac{h_{Design}}{b}\right) + 2{,}0\ , \quad (9)$$

$$Y_{e-o} = \left(K_\phi * K_F * K_h * K_\sigma * K_I\right) * h_{Design} + 2{,}0\ , \quad (10)$$

The lahar hydrodynamic pressure (p_w) is estimated with the AASHTO model (2012). The model considers a triangular distribution of this pressure, taking a value of zero in the deepest point and a maximum value in the flow surface. The hydrodynamic pressure is a function of the specific weight of the flow, its velocity and the accumulation of debris (C_D).

$$p_{w,max} = C_D * \frac{\gamma_{Lahar}}{g} * {v_{Lahar}}^2\ , \quad (11)$$

The model of Haehnel and Daly (2004) is used to quantify the impact of the debris (F_i) on piers or abutments. This model assesses the impact force through a one-degree-of-freedom system assuming a rigid structure. Thus, the impact force is based on the flow velocity (v_{Lahar}), the mass of debris (m_d) and the effective contact stiffness of the collision ($\hat{k}$):

$$F_i = v_{Lahar} * \sqrt{\hat{k} * m_d}\ , \quad (12)$$

Nat. Hazards Earth Syst. Sci. Discuss., https://doi.org/10.5194/nhess-2017-330
Manuscript under review for journal Nat. Hazards Earth Syst. Sci.
Discussion started: 12 October 2017

Natural Hazards and Earth System Sciences
Discussions
Open Access
EGU

4.2 Values of the variables involved in the limit state functions

In order to quantify the independent variables of the limit state function, the first step is to define the nature of the variables, based on their uncertainty degree. This system presents random variables associated to lahar hazard, such as lahar density and debris accumulation. To quantify these variables, probability distribution functions are used, based on studies prepared by Chile's National Geology and Mining Service (Sernageomin) (Castruccio et al., 2010; Bono, 2014) and the United States Geological Survey (Pierson et al., 2009; Vallance and Iverson, 2015).

Furthermore, regarding variables associated to the bridge capacity to lahars, random variables are also considered due to the uncertainty in the bridge design. Goodness of fit tests were undertaken to determine the probability functions and the parameters of these variables, using the information from the Chilean bridge inventory and the Highway Manual of the Ministry of Public Works (MOP, 2016). Table 1 summarizes the values of the variables involved in the limit state functions.

Table 1: Variables involved in the limit state functions.

Variable	Name	Unit	Deterministic Value/ Probabilistic Distribution	Value Reference
h_{Lahar}	Lahar Height	m	Lahar Intensity	Hazard Intensity
K_w; K_2; K_ϕ	Flow Skew Factor	-	1,0	Bridge Inventory (MOP)
K_n; K_g; K_d	Granulometric Dispersion Factor	-	1,0	MOP (2016)
K_{gr}	Pier Group Factor	-	Uniform (1,0; 1,9)	MOP (2016)
K_R	Foundation Emergence Factor	-	Triangular (1,0; 1,06; 1,06)	MOP (2016)
h_{Design}	Flow Design Depth	m	Lognormal (1,16; 0,53) - 1,0	Bridge Inventory (MOP)
NP	Number of Lanes	-	Discrete (1-2) (0,578; 0,422)	Bridge Inventory (MOP)
L	Bridge Width	m	Burr (4,5; 14,1; 4,9)	Bridge Inventory (MOP)
b	Column Width	m	Triangular (0,063L; 1,0L; 0,08L)	Bridge Inventory (MOP)
i	Bed Slope in Bridge	-	Uniform (1,0; 1,3)	Bono (2014)
L_{Bridge}	Bridge Length	m	Lognormal (0,78; 2,79)	Bridge Inventory (MOP)
K_1	Pier Shape Factor	-	Triangular (0,65; 1,2; 1,1)	Bridge Inventory (MOP)
K_3	Bed Condition Factor	-	1,1	MOP (2016)
K_E	Debris Accumulation Factor	-	Uniform Discrete (0,21; 0,79)	Zavenbergen et al. (2007)
W_d / b	Debris Width/Pier Width Ratio	-	Normal (15,1; 8,2)	Zavenbergen et al. (2007)
b_F / L_P	Lahar Width/Bridge Length Ratio	-	Uniform (1,22; 1,83)	Self-prepared with historical data
n_{Lahar}	Lahar Roughness Coefficient	-	Triangular (0,020; 0,053; 0,099)	Cowan (1956); Laenen and Hansen (1988)
K_F	Abutment Shape Factor	-	Triangular (0,3; 1,0; 0,75)	Bridge Inventory (MOP)
K_I	Flow Intensity Factor	-	1,0	MOP (2016)
C_D	Drag Coefficient	-	1,4	AASHTO (2012)
γ_{Lahar}	Lahar Specific Weight	N/m^3	Triangular (15.598; 19.031; 19.031)	Pierson et al. (2009)
γ_{Gravel}	Gravel Specific Weight	N/m^3	24.525	Vallance and Iverson (2015)
D_{Gravel}	Gravel Diameter	mm	Triangular (0,031; 32,0; 2,0)	Castruccio et al. (2010)
k	Effective Contact Stiffness	MN/m	14,0	Haehnel and Daly (2004); AASHTO (2012)
h_{imp}	Gravel impact Height	m	Uniform (0; h_{Lahar})	Assumption
e_{Super}	Superstructure Thickness	cm	Gen. Ext. Value (0,3; 4,7; 18,6)	Bridge Inventory (MOP)

Nat. Hazards Earth Syst. Sci. Discuss., https://doi.org/10.5194/nhess-2017-330
Manuscript under review for journal Nat. Hazards Earth Syst. Sci.
Discussion started: 12 October 2017

Natural Hazards and Earth System Sciences
Discussions

5 Calibration y parametrization of bridge fragility curves due to lahars

5.1 Monte Carlo simulations for the calibration of fragility curves

The reliability analysis comprises analytical solution methods and numerical solution methods. The first group features the first-order second-moment (FOSM) method, the first-order reliability method (FORM) and the second-order reliability method (SORM). On the other hand, the numerical solution methods include the Monte Carlo simulation (MCS) and the response surface method (RSM). In this context, Schultz et al. (2010) highlight the use of numerical solution methods, especially the MCS, prevailing over the analytical solution ones, due to the simplifications of the latter. Within these limitations the assumption that the limit state function is linear, the need to assume an explicit correlation structure for basic variables and the limitations with regard to the probability distributions of the random variables are highlighted. Considering this, the MCS method is used to develop bridge fragility curves due to lahars. These allow incorporating the uncertainty of the characteristics of lahars and the structure in the quantification of the bridge failure probability, without the mentioned limitations.

With the limit state functions and variables already defined, the Monte Carlo simulations can be performed. Therefore, a fixed intensity lahar h_1 is considered. The probability distributions of the system's random variables imply the obtainment of different values of limit state functions $g(X)$. If this function is less than zero in a specific simulation, it means that the bridge fails due to a lahar with intensity h_1. The bridge failure probability due to a lahar of intensity h_1 is equal to the sum of the number of simulations where function $g(X)$ is negative, divided by the number of total simulations with this intensity (NS) (Vorogushyn et al., 2009).

$$P_{Failure} = P(g(X) < 0 | H = h_1) = \frac{\sum_{i=1}^{NS} k_i}{NS}, \quad (13)$$

$$k_i = \begin{cases} 1 & si\ g_i(X) < 0 \\ 0 & si\ g_i(X) \geq 0 \end{cases}, \quad (14)$$

Simulations with fixed intensity h_1 will allow quantifying the failure probability associated to the point of the fragility curve with abscissa h_1. This experiment is carried out repeatedly for several intensity levels, with the aim of obtaining the complete fragility curve for each failure mechanism identified. Specifically, 10,000 simulations are performed for each intensity level. The failure probability is quantified for lahar heights discretized every 0.25 m.

5.2 Calibrated bridge fragility curves due to lahars

5.2.1 Fragility curves by bridge failure mechanism

Once defining the supply and demand functions of the failure mechanisms, together with its variables, 10,000 simulations are run for a fixed lahar height level h_1. The percentage of simulations where function $g_{VI}(X)$ is less than zero is equivalent to the overturning probability of the infrastructure in the presence of a lahar of h_1. After doing this for different lahar height

Nat. Hazards Earth Syst. Sci. Discuss., https://doi.org/10.5194/nhess-2017-330
Manuscript under review for journal Nat. Hazards Earth Syst. Sci.
Discussion started: 12 October 2017

Natural Hazards and Earth System Sciences
Discussions

levels, the overturning fragility curves of the piers and abutments are obtained. The same experiment was performed for the function $g_{DS}(X)$ to calibrate the deck sliding fragility curve. Figure 3 shows the fragility curves by bridge failure mechanism.

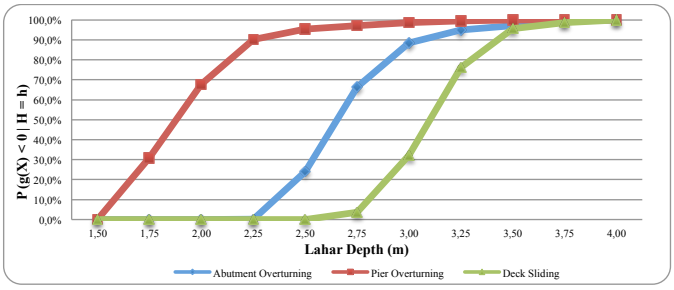

Figure 3: Fragility curves for bridge infrastructure overturning deck sliding due to lahars.

The analysis of infrastructure overturning fragility curves allow concluding that piers are more susceptible to overturn than the abutments in the event of lahar flows. Given any intensity level of the disaster, piers have a greater probability of overturning than the abutments. The analysis of the functional shape of the overturning fragility curves shows that, regarding the abutments, the maximum increase is achieved when the intensity grows from 2.5 to 2.75 m, where the failure probability increases 42.4 %. In the case of piers, the maximum growth of the probability of failure is reached between 1.75 and 2.0 m; increasing 36,8 % the overturning probability.

When analyzing the deck sliding fragility curve, the deck failure probability is zero if the lahar has an intensity less or equal to 2.50 m. This is mainly due to the fact that low-height lahars do not reach the bridge clearance and, consequently, they do not affect the superstructure. Nevertheless, if the intensity of the lahar exceeds this level, the failure probability increases rapidly. The growth rate of this fragility curve also has a maximum, which is reached when the lahar arrives at 3.25 m. Particularly, if the lahar increases from 3.0 to 3.25 m, the sliding probability of the deck increases 43.8 %. This is mainly due to the fact that if the lahar reaches 3.5 m, it already touches the road elevation of most bridges in the inventory.

5.2.2 Fragility curves by bridge categories

The previous analysis allows concluding that a relevant factor in a bridge failure due to a lahar is the presence of piers. Therefore, two bridge categories were defined: bridges without piers (C1) and bridges with piers (C2). The category C1 corresponds to bridges with infrastructure composed only of abutments. On the other hand, the category C2 represents bridges with one or more piers.

Nat. Hazards Earth Syst. Sci. Discuss., https://doi.org/10.5194/nhess-2017-330
Manuscript under review for journal Nat. Hazards Earth Syst. Sci.
Discussion started: 12 October 2017

To obtain the fragility curves for these two bridge categories, each simulation considered that the failure of the bridge occurs when at least one of its components fails. For example, a bridge of category C1 fails when the abutment overturns and/or when the superstructure slides. The same is defined for category C2, where the bridge fails when the pier or abutment overturns and/or the superstructure slides. Figure 4 shows the fragility curves for both bridge categories, in addition to the failure probability of each component in a histogram.

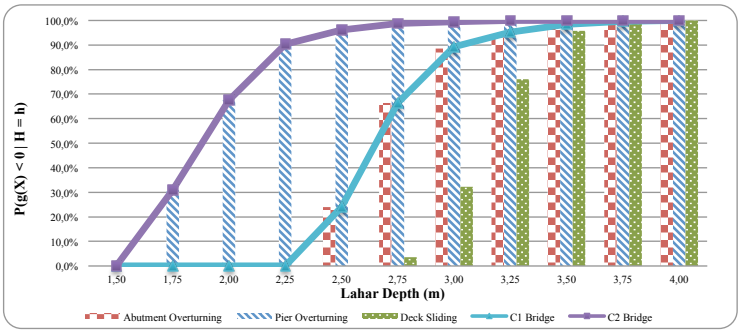

Figure 4: Fragility curves for bridges without piers (C1) and with piers (C2) due to lahars.

Fig. 4 allows concluding that bridges without piers (C1) are stronger than bridges with piers (C2) in the presence of lahar flows. The reason thereof is that piers are more susceptible of overturning than the abutments. In this sense, it can be highlighted that the failure of bridges without piers is guided by the overturning of abutments, while in the bridges with piers, the failure is guided by the overturning of piers. The sliding of the superstructure is not a triggering factor of bridge failures due to lahars.

5.3 Parametrization of bridge fragility curves due to lahars

When considering risk management from a strategic point of view, the parametrization of bridge fragility curves due to lahars entails a series of advantages. It allows directly estimating the failure or collapse probability of each bridge category based on the lahar depth. Moreover, it allows quantifying the failure probability continuously, that is, not every 25 cm of lahar.

For the parametrization of fragility curves, a cumulative lognormal distribution is considered. It has several advantages for modelling the fragility of a given structure. First, this function has a lower bound equal to zero on the x-axis, which implies that there is no damage probability with a lahar of intensity zero. Additionally, Shinozuka et al. (2000) and Lallemant et al. (2015) highlight that when a variable or fragility curve with a lognormal distribution is multiplied or divided by a safety factor, which has a lognormal distribution, the resulting fragility curve also has a lognormal distribution.

When assessing parameters μ and β of the cumulative lognormal distribution reflecting the fragility curve, the bridge failure

Nat. Hazards Earth Syst. Sci. Discuss., https://doi.org/10.5194/nhess-2017-330
Manuscript under review for journal Nat. Hazards Earth Syst. Sci.
Discussion started: 12 October 2017

probability associated to a lahar of intensity h_i can be estimated through the following equation:

$$P(g(X) < 0 | H = h_i) = \Phi\left(\frac{\ln(h_i) - \mu}{\beta}\right), \quad (15)$$

The method of maximum likelihood estimation (MLE) was used for the parametrization of fragility curves. This tool allows determining the distribution parameters that maximize the occurrence probability of data obtained in the Monte Carlo simulations. In this case, the objective of the MLE is to determine the value of the bridge failure probability (p_i) due to a lahar of intensity h_i that maximizes the probability of obtaining the pairs (n_i, N_i) associated to the simulations of all lahar intensity levels h_i. This is obtained by maximizing the likelihood function, which is equal to the product of the binomial probabilities for each height level h_i.

$$Likelihood = \prod_{i=0}^{4,0} P(n_i \; in \; N_i \; collapse | H = h_i) = \prod_{i=0}^{4,0} \binom{N_i}{n_i} * {p_i}^{n_i} * (1 - p_i)^{N_i - n_i}, \quad (16)$$

Considering a fragility curve with cumulative lognormal distribution, p_i is replaced by the function of the cumulative lognormal, and parameters μ and β are estimated. In this case, it is best to maximize the likelihood logarithm instead of the likelihood function. Thus, the parameters of the cumulative lognormal distribution are obtained through the following expression proposed by Lallemant et al. (2015):

$$\hat{\mu}, \hat{\beta} = argmax_{\mu,\beta} \sum_{i=0}^{4,0} \left[n_i * ln\left(\Phi\left(\frac{\ln(h_i) - \mu}{\beta}\right)\right) + (N_i - n_i) * ln\left(1 - \Phi\left(\frac{\ln(h_i) - \mu}{\beta}\right)\right)\right], \quad (17)$$

These parameters were obtained by iterating their values and finding the combination that maximizes Eq. (17). The process was carried out for bridges without piers (C1) and bridges with piers (C2). For bridges without piers (C1), the result was that the likelihood function is maximized with μ equal to 0.98 and β equal to 0.09. In this manner, it is concluded that the failure height of bridges without piers due to lahars has a cumulative lognormal distribution ($\mu = 0.98; \beta = 0.09$). Regarding the bridges with piers, it was concluded that the collapse height of the C2 bridges due to lahars has a cumulative lognormal distribution with μ equal to 0.63 and β equal to 0.14. Fig. 5 shows both the analytical fragility curve and the parametrized curve of the bridges without piers (C1) and with piers (C2).

Nat. Hazards Earth Syst. Sci. Discuss., https://doi.org/10.5194/nhess-2017-330
Manuscript under review for journal Nat. Hazards Earth Syst. Sci.
Discussion started: 12 October 2017

Natural Hazards and Earth System Sciences
Discussions

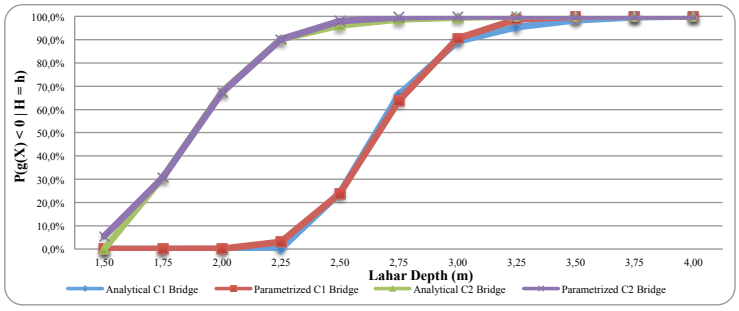

Figure 5: Analytical and parametrized fragility curves of bridges without piers (C1) and with piers (C2) due to lahars.

6 Validation of bridge fragility curves due to lahars and analysis of results

6.1 Validation of bridge fragility curves due to lahars

The fragility curves were calibrated based on physical models and expressions recommended in the literature; for example, the equations given by the Highway Manual of the Chilean Ministry of Public Works (MOP, 2016) for estimating the scour supply in order to design bridges. Likewise, the expressions of HEC-18 (Arneson et al., 2012) for quantifying the scour demand of the flows. All this requires the validation of the developed analytical models.

Parametrized fragility curves allow quantifying the analytical failure probability of a bridge from a specific category (C1 or C2), subjected to a lahar of a specific intensity measured as depth (h_{Lahar}). In order to validate parametrized fragility curves, this analytical probability value is statistically compared with the empirical failure probability. The latter is estimated as the proportion of bridges of each category reached and destroyed by historical lahars of depth h_{Lahar}.

Thus, for the validation, empirical points of the fragility curve are estimated, which are subsequently compared with the analytical fragility curves. The mapping of empirical points uses the damage attributes and records of lahars produced during the eruptions of the Villarrica Volcano in 1964, 1971 and 2015, and the Calbuco Volcano in 1961 and 2015. The built empirical points are based on evidence provided by Klohn (1963), Naranjo and Moreno (2004), Moreno, Naranjo and Clavero (2006), MOP (2015a), MOP (2015b) and Flores (2016).

In order to statistically compare the analytical and empirical failure probabilities, consecutive z-tests were performed, which allow determining whether the difference between two proportions is significant. For this, the following hypothesis were defined for each empirical point:

$$H_0: p_a = p_e \quad vs \quad H_a: p_a \neq p_e \,, \tag{18}$$

Where p_0 corresponds to the analytical probability of the point obtained through the parametrization.

Nat. Hazards Earth Syst. Sci. Discuss., https://doi.org/10.5194/nhess-2017-330
Manuscript under review for journal Nat. Hazards Earth Syst. Sci.
Discussion started: 12 October 2017

Natural Hazards and Earth System Sciences
Discussions

Considering the defined hypothesis, test statistic Z is given by the following expression:

$$Z = \frac{(\hat{p}_a - \hat{p}_e)}{\sqrt{\hat{p} * (1-\hat{p}) * \left(\frac{1}{n_a} + \frac{1}{n_e}\right)}} \sim Normal(0,1)\ , \tag{19}$$

$$\hat{p} = \frac{x_a - x_e}{n_a + n_e}, \tag{20}$$

The results of the test statistic Z and the p-value obtained for each hypothesis test associated to each point are shown in the following tables:

Table 2: Validation data for fragility curves of bridges without piers (C1).

Nº	h (m)	Bridges without piers (C1)			
		p_a	p_e	Z	p-value
1	1,50	0,0 %	0,0 %	0,00	50,0 %
2	2,50	24,0 %	50,0 %	0,86	19,5 %
3	3,50	99,9 %	100,0 %	0,03	48,8 %
4	3,75	100,0 %	100,0 %	0,00	50,0 %
5	4,00	100,0 %	100,0 %	0,00	50,0 %
6	5,00	100,0 %	100,0 %	0,00	50,0 %
7	6,75	100,0 %	100,0 %	0,00	50,0 %

Table 3: Validation data for fragility curves of bridges with piers (C2).

Nº	h (m)	Bridges with piers (C2)			
		p_a	p_e	Z	p-value
1	1,50	5,4 %	0,0 %	-0,24	40,5 %
2	3,50	100,0 %	100,0 %	0,00	50,0 %
3	3,75	100,0 %	100,0 %	0,00	50,0 %
4	6,75	100,0 %	100,0 %	0,00	50,0 %

Once the p-value of every hypothesis test associated to each point is calculated, it is compared with a significance level α for validation. If the p-value is less than the defined significance level α, the null hypothesis H_0, stating that the bridge empirical failure probability due to lahars is equal to that obtained by the parametrization ($H_0: p_a = p_e$), should be rejected with that significance level. Thus, the critical case entailed by the rejection of the null hypothesis is when the p-value is lower.

In this case, the lower p-value (19.5 %) is given by point 1 of bridges C1, where a lahar with a height of 2.50 m results in an analytical probability of 24.0 % and an empirical probability of 50.0 %. It is therefore concluded that it is not possible to reject the null hypothesis H_0, which establishes that empirical bridge failure probability due to lahars is equal to that indicated by the analytical model, with a 5 % significance level.

Nat. Hazards Earth Syst. Sci. Discuss., https://doi.org/10.5194/nhess-2017-330
Manuscript under review for journal Nat. Hazards Earth Syst. Sci.
Discussion started: 12 October 2017

Natural Hazards and Earth System Sciences
Discussions

6.2 Analysis of validated fragility curves and failure model

Once the bridge fragility curves due to lahars are calibrated, parametrized and validated, the main results obtained in the research are analyzed. First, it should be highlighted that the minimum p-value obtained is higher than 10 %, thus obtaining a satisfactory validation of the fragility curves. This allows inferring that the bridge failure model due to lahars proposed in the free-body diagram allows representing the fragility of its components in the presence of these flows. Furthermore, it is deduced that the modelling method based on the reliability theory and the Monte Carlo simulations can be used for calibrating the bridge fragility curves due to lahars. Likewise, the satisfactory validation allows inferring that the existing models integrated in the limit state functions and the values of the used variables reflect the stability of the bridge due to a lahar flow. Finally, the validation of the parametrized fragility curves allow inferring that the cumulative lognormal distribution with the parameters obtained through the MLE represent the bridges' fragility in case of lahars.

On the other hand, the analysis of the models and equations used in the limit state functions allow concluding that the lahar depth is the main variable in the quantification of lahar loads and bridge capacity to these flows. The lahar velocity, the scour demand, the hydrodynamic pressure and the height of the debris impact depend on the flow height. Thus, it is concluded that this variable can be used to represent the hazard intensity in the fragility curves associated to lahars.

Regarding the simulations of calibrated fragility curves for the overturning of piers and abutments, the greater contribution of the moment associated to the hydrodynamic pressure with respect to the debris impact, can be highlighted. It is observed that the average impact moment does not exceed 0.18 % of the hydrodynamic moment in the case of piers, and 0.37 % for abutments. Moreover, it should be noted that the contribution percentage of the impact moment decreases as the lahar height increases.

Concerning the deck sliding, it is important to indicate that the net force is kept relatively constant when the lahar intensity is lower or equal to 2.5 m. This is because the tangential force of the lahar on the superstructure is null. Afterwards, when the lahar reaches the beams and decks, the average, minimum and maximum net forces start to decrease. For example, the average net force is negative when the lahar height is higher or equal to 3.25 m, where the failure probability is 76.1%. Moreover, if a lahar has an intensity higher or equal to 4.0 m, the deck has a 100 % probability of sliding, because the maximum net force of the simulations is negative.

Furthermore, it is found that the contribution of the debris impact force on the superstructure is lower in relation to the hydrodynamic force. In this particular case, the maximum average impact force reaches 0.61 % of the hydrodynamic force. The reason is that the impact of debris on the superstructure is infrequent, since it requires the height of the impact to be higher than the height of the infrastructure, but lower than the cross-section elevation. Nevertheless, if such impact should occur, the impact force would be high.

Regarding the fragility curves by bridge categories, the failure of bridges from category C2 is mainly due to the overturning of piers. In fact, when the lahar height is less or equal to 2.0 m, the pier is the only triggering component, because the other ones have no failure probability. The failure of the abutments starts from 2.25 m of the lahar; however, at that level, the pier

already has a failure probability of 90.2 %, which means that the influence of the abutment on the bridge failure is lower. That is why the fragility curve of C2 bridges is similar to that of the overturning of piers.

Something similar occurs in the bridges without piers (C2). In this case, the triggering component is the abutment, because it is more vulnerable than the deck to lahars. When the flow depth is higher than 2.25 m and lower than 2.5 m, the C1 bridge can fail only if the abutments overturn, since the sliding probability of the deck is zero. The latter is no longer null at 2.75 m, reaching a sliding probability of just 3.6 %, compared with an abutment overturning probability of 66.4 %. Therefore, the abutment is always the main failure factor in this type of bridges.

7 Conclusions and recommendations

In this paper a bridge failure model and bridge fragility curves due to lahars are proposed, considering piers and abutments overturning, as well as, deck sliding. Models development consider the calibration, parametrization and validation of bridge fragility curves due to lahars based on a limit state model. Two types of bridges are considered in the analysis, this is, bridges with and without piers. Monte Carlo simulations are applied to estimate the probability of failure given by different lahar depths. Fragility curves of bridges are parameterized by maximum likelihood estimation, using a cumulative lognormal distribution. Parametrized fragility curves were satisfactorily validated using empirical data with a confidence level of 95 %. Thus, through the empirical validation it is concluded that the models included in the limit state functions and the proposed values to characterize lahar flows are representative to prevailing loads and bridge capacity.

From the analysis of validated fragility curves, it was concluded that decks fail due to infrastructure overturning prior to sliding. The deck sliding probability ceases to null (3.6 %) when the height of the lahar is equal to 2.75 m. In the presence of a lahar of this intensity, the piers and abutments overturning probabilities are 97.2 % and 66.4 %, respectively. This implies that the probability that the deck fails and that the infrastructure does not fail is 0.03 %. In addition, it was concluded that bridges with piers are more vulnerable to lahar flows compared to bridges without piers. The most evident difference between these bridges was obtained in the lahars of height 2.25 m. Given this intensity, bridges without piers have a 0.1 % probability of failure while those with piers have a 90.3 % probability of failure. This result was expected because piers are more susceptible to overturn than abutments due to lahars. With the developed fragility curves, agencies can determine the failure probability of bridges due to a lahar presenting a specific depth. The proposed failure model can be adapted and calibrated to bridge designs different to the structures accounted in the article. When required, the supply function considered in the model can be conditioned to local bridge design standards and adjusted accordingly.

For the application of these models it is recommended that expected hazard scenarios, in terms of recurrence and intensity, are first simulated. The resulting hazard intensity can then be estimated for the affected network, in particular exposed bridges, and their failure probability can be consequently calculated. Further research is being held in this regard, where a computational platform is being developed for the consistent application of the developed fragility curves to existing exposed networks. With this, local authorities can review their road and bridge designs and existing infrastructure in order to

assess and apply mitigation strategies prior the occurrence of a volcanic event. In this regard, the vulnerability of culvert to lahars should also be incorporated into risk assessment.

Acknowledgements

The authors acknowledge the National Commission for Scientific and Technological Research (CONICYT), which has financed the FONDEF Project ID14I10309 Research and Development of Models to Quantify and Mitigate the Risk of Natural Hazards in the National Road Network. Likewise, they express their gratitude to all the institutions that participated and contributed to this project, especially the Research Center for Integrated Disaster Risk Management CONICYT/FONDAP/15110017 (CIGIDEN), the Road Department of the Chilean Ministry of Public Works and the National Geology and Mining Service of the Chilean Ministry of Mining, the National Emergency Office of the Ministry of Interior and Public Security (ONEMI) and the Gremial Association of Concessionaires (COPSA).

References

American Association of State Highway and Transportation Officials: LRFD bridge design specifications, AASHTO, Washington D.C., United States, 2012.

Arneson, L., Zevenbergen, L., Lagasse, P. and Clopper, P.: Evaluating scour at bridges: Hydraulic Engineering Circular Nº18, Federal Highway Administration Publications, Washington D.C., United States, 2012.

Blong, R. J.: Volcanic hazards: a sourcebook on the effects of eruptions, Academic Press, Sidney, Australia, 1984.

Bono, L.: Modelación de los lahares del Volcán Villarrica en el sector de Pucón, Región de la Araucanía, Memoria de Título, Universidad de Chile, Santiago, Chile, 2014.

Breusers, H., Nicollet, G. and Shen, H.: Local scour around cylindrical piers, J. Hydraul. Res., 15, 211-252, 1977.

Castruccio, A., Clavero, J. and Rivera, A.: Comparative study of lahars generated by the 1961 and 1971 eruptions of Calbuco and Villarrica volcanoes, Southern Andes of Chile, J. Volcanol. Geoth. Res., 190, 297-311, 2010.

Cowan, W.: Estimating hydraulic roughness coefficients, Agr. Eng., 37, 473-475, 1956.

Federal Emergency Management Agency: Flood model: HAZUS-MH MR3 technical manual, FEMA, Washington D.C., United States, 2011.

Flores, F.: Dynamics of 2015 Villarrica and Calbuco lahar flows, in: Cities on Volcanoes 9, Servicio Nacional de Gelogía y Minería, Puerto Varas, Chile, 2016.

Haehnel, R. and Daly, S.: Maximum impact force of woody debris on floodplain structures, J. Hydraul. Eng., 130, 112-120, 2004.

Kaye, G. D.: Volcanic hazard risk assessment for the RiskScape program, with test application in Rotorua, New Zealand, and Mammoth Lakes, USA, Ph.D. thesis, University of Canterbury, Christchurch, New Zealand, 2008.

Klohn, E.: The february 1961 eruption of Calbuco Volcano, B. Seismol. Soc. Am., 53, 1435-1436, 1963.

Laenen, A. and Hansen, R. P.: Simulation of three lahars in the Mount St. Helens area, Washington, using a one-dimensional unsteady state streamflow model, U.S. Geological Survey, Portland, United States, 1988.

Lallemant, D., Kiremidjian, A. and Burton, H.: Statistical procedures for developing earthquake damage fragility curves, Earthq. Eng. Struct. D., 44, 1373-1389, 2015.

Lara, L. E., Orozco, G., Amigo, A. and Silva, C.: Peligros volcánicos de Chile: Carta geológica de Chile, in: Serie Geología Ambiental, Servicio Nacional de Geología y Minería, Santiago, Chile, 2011.

Leonard, G. S., Johnston, D. M., Williams, S., Cole, J. W., Finnis, K. and Barnard, S.: Impacts and management of recent volcanic eruptions in Ecuador: lessons for New Zealand, GNS Science Report 2005/20, 2005.

Ministerio de Obras Públicas: Minuta emergencia Volcán Villarrica: Región de La Araucanía, in: Emergencia Volcán Villarrica 2015, Temuco, Chile, April 2015, 2015a.

Ministerio de Obras Públicas: Minuta emergencia Volcán Calbuco: Región de Los Lagos, in: Emergencia Volcán Calbuco 2015, Puerto Montt, Chile, June 2015, 2015b.

Ministerio de Obras Públicas: Volumen 3: Instrucciones y criterios de diseño, in: Manual de Carreteras, Ministerio de Obras Públicas, Volumen 3, Santiago, Chile, 2016.

Moreno, H., Naranjo, J. and Clavero, J.: Generación de lahares calientes en el volcán Calbuco, in: XI Congreso Geológico Chileno, Universidad Católica del Norte, Antofagasta, Chile, 7-11 August 2006, 513-516, 2006.

Moreno, H.: El Volcán Villarrica y su actividad, Servicio Nacional de Geología y Minería, Pucón, Chile, 2015.

Mueller, D.: Local scour at bridge piers in nonuniform sediment under dynamic conditions, Ph.D. thesis, Colorado State University, Colorado, United States, 1996.

Muñoz-Salinas, E., Manea, V. C., Palacios, D. and Castillo-Rodríguez, M.: Estimation of lahar flow velocity on Popocatepetl volcano (Mexico), Geomorphology, 92, 91-99, 2007.

Nairn, I. A.: The effects of volcanic ash fall (tephra) on road and airport surfaces, Institute of Geological & Nuclear Sciences, Lower Hutt, New Zealand, 2002.

Naranjo, J. A. and Moreno, H.: Laharic debris-flows from Villarrica volcano, in: Boletín Servicio Nacional de Geología y Minería, 61, Santiago, Chile, 28-38, 2004.

National Cooperative Highway Research Program: NCHRP Report 653: Effects of debris on bridge pier scour, Transportation Research Board, Washington D.C., United States, 2010.

Parfitt, E. A. and Wilson, L.: Fundamentals of physical volcanology, Blackwell Publishing, Massachusetts, United States, 2008.

Pierson, T.: Initiation and flow behavior of the 1980 Pine Creek and Muddy River lahars, Mount St Helens, Washington, Geol. Soc. Am. Bull., 96, 1056-1069, 1985.

Pierson, T., Scott, W. and Vallance, J.: Eruption-related lahars and sedimentation response downstream of Mount Hood: Field guide to volcaniclastic deposits along the Sandy River, Oregon, in: Volcanoes to Vineyards: Geologic Field Trips

through the Dynamic Landscape of the Pacific Northwest, The Geological Society of America, Seattle, United States, 221-236, 2009.

Rossetto, T., Ioannou, I. and Grant, D. N.: Existing empirical vulnerability and fragility functions: compendium and guide for selection, GEM Technical Report 2013-X: GEM Foundations, Pavia, Italy, 2013.

Schultz, M. T., Gouldby, B. P., Simm, J. D. and Wibowo, J. L.: Beyond the factor of safety: developing fragility curves to characterize system reliability. U.S. Army Corps of Engineers (USACE): Engineer Research and Development Center (ERDC SR-10-1), Washington D.C., United Sates, 2010.

Shinozuka, M., Feng, M., Lee, J. and Naganuma, T.: Statistical analysis of fragility curves, J. Eng. Mech., 126, 1224-1231, 2000.

Smith, G. A. and Fritz, W. J.: Volcanic influences on terrestrial sedimentation, Geology, 17, 375-376, 1989.

Tsubaki, R., Ichii, K., Bricker, J. D. and Kawahara, Y.: Development of fragility curves for railway ballast and embankment scour due to overtopping flood flow, Nat. Hazard Earth Sys., 16, 2455-2472, 2016.

Vallance, J. and Iverson, R.: Lahars and their deposits, in: The Encyclopedia of Volcanoes, 2nd Edition, Elsevier, San Diego, United States, 649-664, 2015.

Vorogushyn, S., Merz, B. and Apel, H.: Development of dike fragility curves for piping and micro-instability breach mechanisms, Nat. Hazard Earth Sys., 9, 1383-1401, 2009.

Waitt, R. B.: Lahar, in: Encyclopedia of Natural Hazards, Springer, Dordrecht, Netherlands, 579-580, 2013.

Wilson, T. M., Stewart, C., Sword-Daniels, V., Leonard, G., Johnston, D.M., Cole, J.W., Wardman, J., Wilson, G., Barnard, S.: Volcanic ash impacts on critical infrastructure, Phys. Chem. Earth, 45, 5-23, 2012.

Wilson, G., Wilson, T., Deligne, N. and Cole, J.: Volcanic hazard impacts to critical infrastructure: A review, J. Volcanol. Geoth. Res., 286, 148-182, 2014.

Zevenbergen, L., Lagasse, P. and Clooper, P.: Effects of debris on bridge pier scour, in: World Environmental and Water Resources Congress 2007: Restoring our Natural Habitat, Environmental and Water Resources Institute of ASCE, Tampa, United States, 15-19 May 2007, 2007.